

# Genetic Distinctions Between Reticular Pseudodrusen and Drusen: Insights from a Genome-Wide Association Study

Roy Schwartz<sup>1,2</sup>, Alasdair N. Warwick (joint first authors)<sup>1,3</sup>, Anthony P. Khawaja<sup>5</sup>, Robert Luben<sup>5,6</sup>, Hagar Khalid<sup>1</sup>, Sumita Phatak<sup>1</sup>, Mahima Jhingan<sup>1</sup>, Coen de Vente<sup>7,8</sup>, Philippe Valmaggia<sup>5,9,10</sup>, Sandra Liakopoulos<sup>11,12</sup>, Abraham Olvera-Barrios<sup>1,13</sup>, Clara I. Sánchez<sup>7,8</sup>, Catherine Egan<sup>1,5</sup>, (joint last authors) Roberto Bonelli<sup>4</sup>, Adnan Tufail<sup>1,5</sup>

<sup>1</sup> Moorfields Eye Hospital NHS Foundation Trust, London, UK

<sup>2</sup> Institute of Health Informatics, University College London, London, UK

<sup>3</sup> University College London Institute of Cardiovascular Science, London, UK

<sup>4</sup> Lowy Medical Research Institute, La Jolla, CA 92037, USA

<sup>5</sup> NIHR Biomedical Research Centre, Moorfields Eye Hospital NHS Foundation Trust & UCL Institute of Ophthalmology, London, UK

<sup>6</sup> MRC Epidemiology Unit, University of Cambridge, Cambridge, UK

<sup>7</sup> Quantitative Healthcare Analysis (qurAI) Group, Informatics Institute, University of Amsterdam, Amsterdam, Netherlands

<sup>8</sup> Amsterdam UMC location University of Amsterdam, Biomedical Engineering and Physics, Amsterdam, Netherlands

<sup>9</sup> Department of Biomedical Engineering, University of Basel

<sup>10</sup> Department of Ophthalmology, University Hospital Basel

<sup>11</sup> Cologne Image Reading Center, Department of Ophthalmology, Faculty of Medicine and University Hospital Cologne, University of Cologne, Cologne, Germany

<sup>12</sup> Department of Ophthalmology, Goethe University, Frankfurt, Germany

<sup>13</sup> Institute of Ophthalmology, University College London

## Abstract

**Purpose:** To explore genetic determinants specific to reticular pseudodrusen (RPD), and to compare these with genetic associations for drusen.

**Setting:** Participants with RPD, drusen, or controls from the UK Biobank (UKBB), a large, multisite, community-based cohort study.

**Methods:** A previously validated deep learning framework was deployed on 169,370 optical coherence tomography (OCT) volumes from the UKBB to identify cases with RPD and/or drusen and controls without these phenotypes. Cases were included if they were 60 years or older, with at least 5 lesions. Five retina specialists manually validated the cohorts using OCT and color fundus photographs. Quantifications of RPD and drusen derived by the framework were used as variables. Two primary genome-wide association study (GWAS) analyses were performed to explore potential genetic associations with number of RPD and drusen within 'pure' cases, where only RPD or drusen were present in either eye. A candidate approach was furthermore adopted to assess 46 previously known AMD loci. Secondary GWAS were undertaken for number of RPD and drusen in mixed cases, as well as binary case-control analyses for pure RPD and pure drusen. Genome-wide significance was defined as  $p < 5e-8$ .

**Results:** A total of 1,787 participants were identified and analysed, including 1,037 controls, 361 pure drusen, 66 pure RPD and 323 mixed cases. The primary pure RPD GWAS yielded four genome-wide significant loci: rs11200630/*ARMS2-HTRA1* ( $p=1.9e-09$ ), rs79641866/*PARD3B* on chromosome 2 ( $p=1.3e-08$ ), rs143184903/*ITPR1* on chromosome 3 ( $p=8.1e-09$ ), and rs76377757/*SLN* on chromosome 11 ( $p=4.3e-08$ ). The latter three are all uncommon variants (minor allele frequency  $< 5\%$ ). A significant association at *CFH* was also observed adopting a candidate approach ( $p=1.8e-04$ ).

Two loci reached genome-wide significance for the primary pure drusen GWAS: rs10801555/*CFH* on chromosome 1 ( $p=6.0e-33$ ) and rs61871744/*ARMS2-HTRA1* on chromosome 10 ( $p=4.2e-20$ ). For the mixed RPD and drusen secondary analyses, lead variants at both the *CFH* and *ARMS2-HTRA1* loci reached genome-wide significance, with *C2-CFB-SKIV2L* additionally associated for mixed drusen alone. Findings from the binary case-control GWAS for drusen mirrored those of the primary drusen analysis, however no variants reached genome-wide significance in the case-control RPD GWAS.

**Conclusions:** Our findings indicate a clear association between the *ARMS2-HTRA1* locus with higher RPD load. Although the association at the *CFH* locus did not reach genome-wide significance, we observed a suggestive link. We furthermore identified three novel associations that are unique to RPD, albeit for uncommon genetic variants. These findings were only observable when quantifying RPD load as a continuous trait, which increased the study's statistical power. Further studies with larger sample sizes are now required to explore the relative contributions of *ARMS2-*

*HTRA1* and *CFH* to RPD development, and to explore the validity of these newly presented RPD-specific genetic associations.

## Introduction

Age-related macular degeneration (AMD) is the leading cause of severe, irreversible vision loss in Europe and North America. It predominantly affects older individuals and can lead to central vision loss by affecting the macula, an area of the retina that is important for detailed visual tasks such as reading and facial recognition.

Traditionally, the presence of drusen - acellular, lipid-rich deposits beneath the retinal pigment epithelium (RPE), characterizes AMD.<sup>1,2</sup> As a result of advancements in retinal imaging, reticular pseudodrusen (RPD), also known as subretinal drusenoid deposits (when detected on optical coherence tomography (OCT) scanning), have been identified as another manifestation of the AMD spectrum.

Several lines of evidence highlight the distinctions between drusen and RPD. Anatomically, drusen are situated beneath the retinal pigment epithelium (RPE), whereas RPD are located above it.<sup>3</sup> Additionally, their biochemical compositions vary: drusen comprise both esterified and non-esterified cholesterol, while RPD predominantly contain unesterified cholesterol.<sup>4</sup> In addition, a recent study showed that RPD are abundant in lysolipids, that are not found in drusen.<sup>5</sup> Numerous studies indicate that the presence of RPD in eyes with AMD increases the risk of rapid progression to late AMD stages, including geographic atrophy (GA) and neovascularisation (mostly type 3 macular neovascularization (MNV)) compared to drusen without RPD.<sup>6,7</sup> Our research has also discovered a correlation between a higher load of RPD and stroke,<sup>8</sup> and other studies have suggested links between RPD and coronary artery disease, as well as lower levels of high-density lipoprotein (HDL).<sup>9</sup> In contrast, large studies have not consistently found these cardiovascular associations with drusen-associated AMD.<sup>10-12</sup> Moreover, meta-analyses have not confirmed a link between AMD and cardiovascular diseases or stroke.<sup>13,14</sup> RPD can also appear in conditions where drusen are not part of the main phenotype, such as pseudoxanthoma elasticum<sup>15</sup>, Late-Onset Retinal Degeneration,<sup>16</sup> and vitamin A deficiency.<sup>17</sup>

Approximately 46-71% of AMD variation is estimated to be heritable.<sup>18</sup> The largest single genome-wide association study (GWAS) to date in AMD identified 52 independently associated common and rare variants distributed across 34 loci.<sup>19</sup> Chief among them is complement factor H (CFH) on chromosome 1, identified as a genetic contributor to AMD in the earliest studies.<sup>20-24</sup> Another major susceptibility locus is the *ARMS2-HTRA1* region on chromosome 10.<sup>25-27</sup> In combination, these two loci are estimated to account for more than half the genetic predisposition to AMD.<sup>28,29</sup>

The genetic basis of RPD is not as well characterized. Previous studies examining RPD genetics have been small and focused only on known AMD-associated risk loci.

The most consistently associated loci for RPD are *ARMS2-HTRA1* followed by *CFH*, although conflicting effect directions have been reported for the latter (Supplementary Table 1).<sup>9,30–43</sup>

Given the differences between RPD and drusen, we theorized that RPD and drusen arise from both shared and distinct biological pathways. Identifying pathways that are unique to RPD could aid in developing targeted therapies. To test this theory, we conducted a GWAS using retinal imaging data from the UK Biobank (UKBB) study, leveraging a validated AI algorithm to identify and quantify drusen and RPD on this large dataset.<sup>44</sup> Our aim was to explore potential genetic associations that are specific to RPD and compare them with associations found for drusen.

## Methods

### UK Biobank

The UKBB study is a large, multisite, community-based cohort study designed to advance the prevention, detection, and treatment of a wide range of severe and potentially fatal diseases. This study contains data from 500,000 predominantly self-described white ethnicity volunteers, aged between 40 and 69, recruited across the United Kingdom between 2006 and 2010.

Eligibility for the study was extended to all UK residents within the specified age group who were registered with the National Health Service (NHS) and resided within a 25-mile radius of any of the 22 assessment centers. The study was approved by the North West Multi-centre Research Ethics Committee (REC reference number: 06/MRE08/65, UKBB project ID 60078), adhering to the principles of the Declaration of Helsinki ([www.ukbiobank.ac.uk](http://www.ukbiobank.ac.uk)). Participants who withdrew their consent were excluded from the study.

A sub-cohort of 67,687 participants underwent OCT and color fundus photography (CFP) imaging at six centers (Sheffield, Liverpool, Hounslow, Croydon, Birmingham, and Swansea). Images were captured using the Topcon 3D OCT 1000 Mark II (Topcon, Japan) under mesopic conditions without pupil dilation using the 3-dimensional macular volume scan (512 horizontal A-scans/B-scan; 128 B-scans in a 6 × 6-mm raster pattern).

### Study population

The research utilized a deep learning framework to distinguish between subjects with RPD, drusen, and control groups within the UKBB dataset. The specifics of this framework have been outlined in a prior publication.<sup>44</sup> In brief, the process involved an image classifier that filtered out ungradable OCT B-scan volumes. This was followed by a deep ensemble model that detected out-of-distribution data, further eliminating ungradable volumes. Once these volumes were removed, another classifier evaluated the gradable B-scan volumes to categorize subjects into groups

with drusen, RPD, or control groups. The final step of the process employed a semantic segmentation model to quantify the number of RPD and drusen within each B-scan. Of note, although the UKBB contains both CFP and OCT scans for participants with retinal imaging, we chose to analyze only OCT B-scans within the framework given findings from previous studies showing their higher sensitivity for RPD compared with CFP.<sup>45,46</sup> However, CFPs were used in human validation of the framework's output, as detailed below.

The AI framework was applied to the entire UKBB OCT dataset to identify subjects with drusen, RPD, and a control group without either of these phenotypes. The study included subjects identified by the AI framework based on the following criteria: a. Age 60 years or older for all groups; b. At least five instances of RPD or drusen when these phenotypes were present. This requirement was set to rule out cases with minimal lesions, which could be due to natural variation. c. For subjects with drusen, the size of the drusen had to surpass 63 microns in at least one eye. This ensured the exclusion of subjects with only "drupelets" (which in population studies are common features and not shown to increase the risk of progression to late AMD),<sup>1</sup> while including subjects with at least early AMD as per the Beckman classification.<sup>1</sup> To accurately measure the size of drusen, we determined the maximum diameter of drusen in any direction (Feret diameter) on the en face plane.

Two retina specialists (H.K., R.S.) graded the cases identified by the AI framework for the presence of RPD, drusen, or both. Multimodal imaging, including OCT and CFP, was used for validation. Cases with advanced AMD (GA or MNV) were excluded as significant changes in the outer retina from neovascular AMD or GA could affect the accuracy of lesion quantification. Any disagreement between graders was adjudicated by a senior grader (A.T.).

Four retina specialists (A.T., S.P., M.J., R.S.) validated the control group through multimodal imaging assessments, including OCT volumes and CFP, to ensure the absence of drusen and RPD. CFPs complemented OCT scans to detect any drusen or RPD outside the field of view of OCT scans. Subjects with ungradable CFPs or with imaging artifacts that would prevent a confirmation of a subject's control status (e.g., shadowing on CFPs, artifacts affecting the outer retina on OCT) were excluded.

Following grader validation of cases, the number of RPD and drusen identified by the semantic segmentation model on all B-scan in the volumes of both eyes for each patient was summed, representing the total lesion count per patient.

## Genome-wide association study

Full details for genotyping and imputation in the UKBB cohort have been described previously.<sup>47</sup> In brief, genotype calling was performed using two arrays: the UK BiLEVE Axiom array (~50,000 participants) and the UK Biobank Axiom array (~450,000 participants). Marker positions are in GRCh37 coordinates. There were 805,426 markers available in the released data after quality control. Genotype imputation was then performed using a combined Haplotype Reference Consortium



and UK10K reference panel, expanding the number of testable variants to ~96 million.

The following exclusions were applied for sample quality control: individuals with relatedness corresponding to third-degree relatives or closer, excess of missing genotypes or more heterozygosity than expected. The GWAS analysis was furthermore restricted to individuals of European ethnicity only due to the lack of power for other genetic backgrounds. The following exclusions were applied for variant-level quality control: call rate <95%, Hardy-Weinberg equilibrium  $p < 1 \times 10^{-6}$ , posterior call probability <0.9, INFO score <0.9 and minor allele frequency <0.01.

GWAS analyses were performed to assess potential genetic associations with (i) pure RPD (defined as cases with RPD in at least one eye but without drusen in either eye) and (ii) pure drusen (defined as cases with drusen in at least one eye but without RPD in either eye). For each analysis, the study cohort included participants with only the phenotype of interest and control participants, as described earlier. The primary analyses were based on the number of RPD and drusen; the count data, which included zero values for control participants, was standardized by adding one to each value prior to log transforming to achieve normal distributions. Secondary analyses were also performed with the additional inclusion of mixed cases (cases with simultaneous presence of drusen and RPD) for number of RPD and number of drusen, as well as binary case-control analyses for pure RPD and pure drusen compared against controls. All GWAS analyses were conducted using a generalised linear mixed model, adjusting for age, sex and the first ten principal components. Correction for multiple testing was performed by applying a genome-wide significance threshold of  $p < 5 \times 10^{-8}$ .

## Candidate approach

For the two primary GWAS analyses (number of pure RPD and pure drusen), a candidate approach was furthermore adopted based on 34 advanced AMD-associated loci previously reported by Fritsche et al<sup>19</sup> and 12 early AMD loci from Winkler et al.<sup>48,49</sup>. Loci were considered to pass experiment-wise significance at  $p < 0.001$  (0.05/46).

## Number of Pure RPD Post-GWAS analysis

Summary statistics results were investigated using FUMA.<sup>50</sup> The SNP2GENE protocol as used to perform positional and expression quantitative trait locus (eQTL) gene mapping/prioritisation.<sup>50</sup> SNPs in high linkage disequilibrium (LD;  $r^2 > 0.6$ ) with any independent lead variant were positionally mapped to genes located within 10kb. Variants were also mapped to a set of prioritized genes within 1Mb if associated with the expression of those genes in retina (reported in EyeGEx<sup>51</sup>) and blood (reported in eQTLGen<sup>50</sup>).

Novel loci (not previously associated with AMD) were further evaluated by deriving credible sets and annotating these to investigate for variants with functional relevance, as well as assessing for colocalization between the RPD signals with gene expression. A Bayesian fine-mapping approach was used to generate 95%

credible sets of putative causal variants for genome-wide significant loci. Variants within 500 kb of each lead variant were included, applying a prior probability of  $10^{-4}$  for each variant. Fine-mapped variants were retained if they were significantly associated with RPD at  $p < 0.05$  and in linkage disequilibrium with the lead variant at  $r^2 > 0.6$ . The OpenTargets Genetics database was then queried for variant annotation.<sup>52,53</sup> Colocalization between novel RPD-associated loci with gene expression was assessed for all genes within 500kb of each lead variant, for all tissues within the GTEx v8 project with at least one significant *cis*-eQTL for those genes.<sup>54</sup> Overlapping variants within 500kb of each lead variant were included. Results were deemed supportive of colocalization if the maximum probability for PP.H4 (both traits are associated and share a single causal variant) was greater than 0.75.

Previously reported AMD-associated loci (that either reached genome-wide significance or passed the experiment-wise significance threshold with the candidate approach) were assessed for colocalization with AMD, using summary statistics from FinnGenn (H7\_AMD, release 10)<sup>55,56</sup> Variants within 500kb of each lead variant from our RPD GWAS were included.

## Statistical Software

GWAS analyses were performed using REGENIE software to account for relatedness across individuals.<sup>57</sup> Genomic inflation factor and heritability estimates were calculated using the LDSC tool<sup>58</sup> and pre-calculated LD scores for European ancestry.<sup>59</sup> All other statistical analyses were performed in R (R for GNU macOS, Version 4.2.0, The R Foundation for Statistical Computing, Vienna, Austria).<sup>60</sup> The R package coloc[REF] was used for fine-mapping and colocalization analyses.<sup>61–63</sup> Other R packages used included targets<sup>64</sup>, tarchetypes<sup>65</sup>, tidyverse<sup>66</sup>, workflowr<sup>67</sup>, flextable<sup>68</sup>, gtsummary<sup>69</sup> and knitr<sup>70</sup>.

## Results

A total of 1,787 European participants met the study inclusion and quality control criteria, including 1,037 controls with no drusen or RPD, 66 participants with RPD but no drusen ('pure RPD'), 361 participants with drusen but no RPD ('pure drusen'), and 323 participants with a mixture of drusen and RPD. The median (interquartile range) number of lesions in the two pure groups was 91 (39-299) RPD and 201 (94-397) drusen, while for the mixed group there were 73 (31-208) RPD and 233 (96-516) drusen. Demographic characteristics are summarized in **Table 1**.

**Table 1. Demographic characteristics**

	Controls N = 1,037	RPD N = 66	Drusen N = 361	Mixed RPD/drusen N = 323
Age	62.6 (60.7, 65.2)	65.6 (63.2, 68.0)	64.5 (61.6, 66.6)	64.2 (60.8, 66.5)

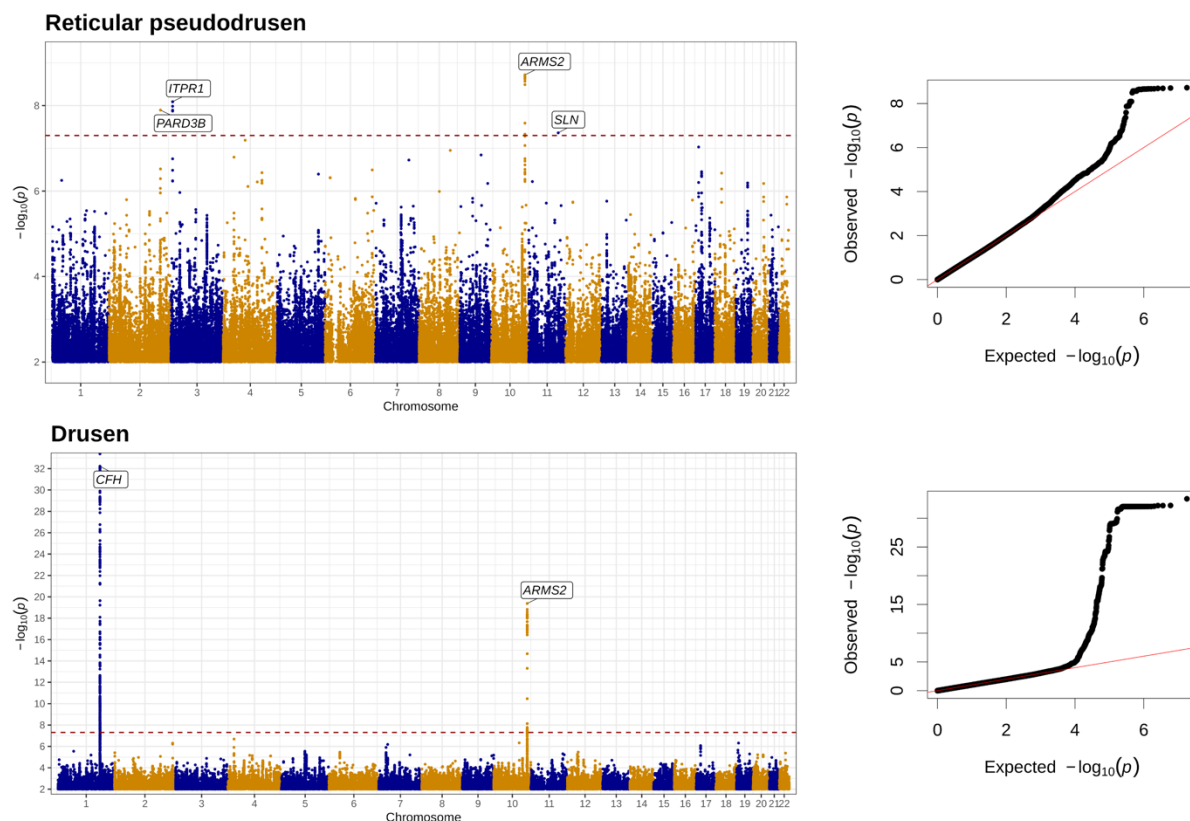
Female	570 (55%)	34 (52%)	216 (60%)	150 (46%)
--------	-----------	----------	-----------	-----------

Age presented as median (interquartile range); sex presented as N (%) female.

## Primary GWAS for number of pure RPD and pure drusen

The primary GWAS analyses yielded 4 loci reaching genome-wide significance for number of pure RPD (*ARMS2-HTRA1*, *PARD3B*, *ITPR1* and *SLN*) and 2 loci for number of pure drusen (*CFH* and *ARMS2-HTRA1*), summarized in **Table 2** and **Figure 2**. We did not observe any inflation of the GWAS statistics (genomic inflation factor = 1.005 and 1.008, RPD and drusen respectively). The estimated SNP heritability for number of RPD was 0.35 (0.41), while that for number of drusen was 0.08 (0.39). Genetic correlation analyses were not possible due to the limited SNP heritability.

**Figure 1. Manhattan and quantile-quantile plots of GWAS results for number of pure RPD (in the absence of drusen) and number of pure drusen (in the absence of RPD)**



Both loci for drusen (*CFH* and *ARMS2-HTRA1*) are well known to be associated with AMD, while among the four found for RPD only the *ARMS2-HTRA1* locus has previously been reported in association with AMD. The lead variants associated with



RPD at *PARD3B* (rs79641866) and *ITPR1* (rs143184903) are both intronic variants, whereas rs76377757 lies in an intergenic region ~8000 base pairs downstream of the *SLN* locus (**Supplementary Figure S1**). It should be noted that the minor allele frequencies for all three novel RPD-associated loci are uncommon (MAF < 0.05).

**Table 2. Genome-wide significant associations with number of pure reticular pseudodrusen and pure drusen.**

	Rs identifier	chr:pos[hg19]	EA/OA (EAF)	Beta (95% CI)	P	Nearest gene
<b>Reticular pseudodrusen</b>						
	rs79641866	2:206022440	T/C (0.03)	0.39 (0.25; 0.53)	1.3e-08	<i>PARD3B</i>
	rs143184903	3:4692390	G/A (0.01)	0.64 (0.42; 0.87)	8.1e-09	<i>ITPR1</i>
	rs11200630	10:124209684	C/T (0.21)	0.16 (0.11; 0.21)	1.9e-09	<i>ARMS2</i>
	rs76377757	11:107598700	T/C (0.01)	0.58 (0.37; 0.79)	4.3e-08	<i>SLN</i>
<b>Drusen</b>						
	rs10801555	1:196660261	A/G (0.46)	0.35 (0.29; 0.41)	6.0e-33	<i>CFH</i>
	rs61871744	10:124203787	C/T (0.24)	0.3 (0.23; 0.37)	4.2e-20	<i>ARMS2</i>

We then adopted a candidate-based approach to look up 34 previously reported AMD-associated variants for AMD and 12 variants for early AMD.<sup>19,48,49</sup> This yielded three additional loci for number of drusen (*C9*, *C3* and *CFI*) and one additional locus for number of RPD (*CFH*) that met the experiment-wise significance threshold ( $p < 0.05/46$ ; **Supplementary Table 2**), all of which have previously been associated with advanced AMD.

## Number of pure RPD post-GWAS analysis

Gene mapping did not prioritise any additional genes at the novel *PARD3B*, *ITPR1* and *SLN* loci. We calculated 95% credible sets at each of the three loci and investigated for any overlap with functional regulatory regions but did not find evidence of this. Colocalization analyses also did not show any evidence for colocalization between these RPD signals with gene expression for any of the tissues with available data from the GTEx database.

Colocalization analyses for previously known AMD loci (*CFH* and *ARMS2-HTRA1*) did, however, show strong evidence for colocalization with AMD GWAS statistics from FinnGen. The estimated posterior probabilities for a shared causal variant between number of pure RPD with AMD were 79% and 100% for *CFH* and *ARMS2-HTRA1*, respectively (**Supplementary Table 3**).

## Secondary GWAS analyses

We subsequently performed GWAS for number of RPD and number of drusen, this time including cases where both RPD and drusen were present (mixed cases). Lead variants at *CFH* and *ARMS2-HTRA1* loci reached genome-wide significance for both analyses, with additional associations near *CFH* at *CFHR4* for mixed RPD, and both *CFHR4* and *CFHR5* for mixed drusen. Furthermore, the *C2-CFB-SKIV2L* locus was genome-wide significant for mixed drusen only (**Supplementary Table 4, Supplementary Figure S2**).

Finally, GWAS analyses were undertaken using binary case-control definitions for pure drusen and pure RPD. Results from the binary pure drusen analysis mirrored those from the primary GWAS for number of pure drusen, with lead variants at both *CFH* and *ARMS2-HTRA1* loci reaching genome-wide significance (**Supplementary Figure S3, Supplementary Table 5**). For the binary pure RPD GWAS however, no variants reached genome-wide significance (**Supplementary Figure S3**).

## Discussion

We present findings from the first reported genome-wide association studies for RPD, confirming an association between *ARMS2-HTRA1*, a known AMD locus, with higher RPD load. In contrast to drusen, *CFH* was not associated with number of RPD at genome-wide significance. However, an association with *CFH* was observed at a less stringent experiment-wise significance threshold and colocalization analyses indicated a shared causal variant for RPD and AMD at this locus. We furthermore identified three novel associations with uncommon lead variants at *PARD3B*, *ITPR1* and *SLN*, although these should be interpreted with caution given the limited power of our study.

The associations between *CFH* and *ARMS2-HTRA1* with AMD are well established, representing the earliest genome-wide significant findings from any GWAS.<sup>20–27</sup> In combination, these two loci are estimated to account for more than half the genetic predisposition to AMD.<sup>28,29</sup> It is striking how the significance of the *CFH* locus, the most significant locus for drusen, is far less significant for RPD. While this is likely in part due to the difference in power, the *ARMS2-HTRA1* locus which is less significant for drusen remains genome-wide significant for RPD. This may suggest that *ARMS2-HTRA1* has a more important role for RPD than *CFH*, but further functional work would be necessary to test this hypothesis. Previous RPD studies have consistently demonstrated an association with *ARMS2-HTRA1*, but reported mixed results for *CFH* (Supplementary Table 1).<sup>71</sup> It is important to recognize the limitations of previous studies, which may explain the discrepancy between previous and current findings, as well as among different previous studies (Supplementary Table 6).

A critical challenge in identifying the genetic origin of RPD relates to the lack of sensitive imaging modalities for large AMD cohorts. Numerous genetic studies

primarily relied on CFP to ascertain the presence of RPD. However, CFP exhibits reduced sensitivity compared to other imaging techniques.<sup>38,39,41,45,46,72</sup>

Consequently, this may lead to an underestimation of RPD prevalence. Our approach involved their identification and quantification on OCT B-scans, which have been shown to have the highest sensitivity (alongside near-infrared (NIR) imaging) for the detection of RPD. Furthermore, the literature reveals a lack of consensus regarding the number of distinct RPD necessary to categorize an eye as RPD-positive. Methodologies range from requiring a single RPD to a minimum of five. The process of retinal aging leads to physiological alterations in the outer retina, which may resemble RPD or drusen in small quantities. Therefore, a more judicious approach in the grading of RPD might entail stipulating a specific number of lesions for a definitive diagnosis. However, only three previous studies had this as a requirement. The detection of RPD in cases of advanced AMD is further complicated due to the extensive retinal damage caused by AMD. Several studies have included such cases. In our study, such cases were excluded.

As an additional limitation, previous research has primarily focused on a select set of known AMD-associated risk loci. This approach overlooks the potential genetic contribution from other AMD risk loci, as well as variants not directly associated with AMD, which could be involved in diverse pathophysiological processes. Given the distinct differences between RPD and drusen, it is plausible that independent and novel pathological pathways may be instrumental in their formation. Therefore, we adopted a hypothesis-free approach to identify genetic associations with RPD.

Similarly, the majority of previous studies were limited by their inclusion of RPD solely in the presence of drusen-associated AMD. Only six of these studies considered pure RPD as part of their analysis, but they were underpowered due to the small number of pure RPD cases (the largest number of pure RPD was 30).<sup>36</sup> Our study has the largest number of pure RPD cases reported in the literature. Another potential difference that could explain our findings is the relatively young age of our pure RPD cohort (mean 65.6 years, compared with an overall mean of 77.5 years in previous studies). The occurrence of RPD at an earlier age may correspond more closely with inheritance, whereas late-onset findings may be more influenced by environmental factors or lifestyle choices that accumulate over time, as well as age-related changes.

The methodology used in our primary analyses differs from the commonly used case-control GWAS study design. Instead, the load of RPD and drusen were used to identify genetic associations, thereby overcoming the low statistical power due to the paucity of cases. Our results indicate that this methodology is valid, given the findings previously known to be associated with these pathologies and found using more traditional techniques. While we could not identify any variants associated with RPD reaching genome-wide significance in a case-control analysis, these associations were exposed when examining the load of RPD.

Our research provides insights into the pathophysiology of RPD. The *ARMS2* gene is expressed in the ellipsoid region of the photoreceptor inner segments,<sup>73</sup> near the subretinal space, where RPD have been observed using OCT and histological analysis, unlike the sub-RPE location of drusen.<sup>3,74</sup> While the exact role of *ARMS2*

remains unknown, it is speculated to be linked to mitochondrial function,<sup>75</sup> extracellular matrix turnover,<sup>76,77</sup> or both. These processes might contribute to photoreceptor damage and cell death, leading to the accumulation of debris identified as RPD.

The close linkage of *HTRA1* with *ARMS2* also may explain the association we observed. The *HTRA1* gene encodes a secreted enzyme that is believed to regulate cell growth and break down various extracellular matrix proteins.<sup>78,79</sup> The AMD risk haplotype is associated with changes in the levels of *HTRA1* expression.<sup>80,81</sup> Therefore, the association between *HTRA1* and RPD might be due to *HTRA1*-mediated increased breakdown of the extracellular matrix, resulting in debris accumulation that appears as RPD.

We also identified three novel loci, not reported previously in association with RPD. It is notable that all three novel variants are uncommon, with a MAF of less than 0.05 and therefore should be interpreted with caution pending validation in larger studies and external validation cohorts. PARD3B (Par-3 Family Cell Polarity Regulator Beta), is predicted to enable phosphatidylinositol binding activity. Additionally, it is predicted to be involved in the establishment of cell polarity and maintenance of epithelial cell apical/basal polarity (strictly apical in many epithelia) and regulated by TGF $\beta$  signalling.<sup>82</sup> Given this role, if PARD3B is involved in the regulation of membrane localization and the organization of cellular components in retinal cells, it could potentially affect where deposits form relative to the RPE, thereby explaining the differential location of RPD compared to drusen.

ITPR1 (Inositol 1,4,5-Trisphosphate Receptor Type 1) encodes an intracellular receptor for inositol 1,4,5-trisphosphate. Upon stimulation by inositol 1,4,5-trisphosphate, this receptor mediates calcium release from the endoplasmic reticulum. ITPR1 plays a role in endoplasmic reticulum stress-induced apoptosis. Mutations in this gene cause spinocerebellar ataxia type 15, spinocerebellar ataxia type 29, as well as Gillespie Syndrome, which may involve iris hypoplasia (verify and add Adnan reference) [Ref RefSeq, Nov 2009].<sup>83,84</sup>

The *SLN* gene encodes sarcolipin, a small proteolipid that regulates several sarcoplasmic reticulum Ca(2+)-ATPases. Sarcoplasmic reticulum Ca(2+)-ATPases are transmembrane proteins that catalyze the ATP-dependent transport of Ca(2+) from the cytosol into the lumen of the sarcoplasmic reticulum in muscle cells. Sarcolipin interacts with Ca(2+)-ATPases and reduces the accumulation of Ca(2+) in the sarcoplasmic reticulum without affecting the rate of ATP hydrolysis.<sup>85</sup>

Early onset drusen maculopathy has been associated with both common and rare, potentially deleterious, genetic variants (with MAF < at 1% level). In a genetic association study, Breuk et al. identified rare variants predominantly involving the complement and lipid metabolism pathways – which were not previously noted in association studies of patients with conventional age of onset AMD.<sup>86</sup> Similarly, patients included in our cohort of pure RPD were much younger than previously studied cohorts of RPD patients, who mostly have the combined RPD and drusen

phenotype. Although these findings should be replicated in a larger cohort of RPD patients, to elucidate their contribution to RPD, the novel genetic associations found may give us insights into pathways and mechanism of RPD formation.

In summary, we present the first reported GWAS for RPD, finding a genome-wide significant association with ARMS2-HTRA1, and potentially novel associations with PARD3B, ITPR1 and SLN. An association with CFH was also observed, though at a lower significance threshold, and this locus colocalized with AMD. Larger studies are needed to clarify the roles of ARMS2-HTRA1 and CFH in RPD development and to validate these newly identified RPD-specific genetic associations. Future research should aim to quantify RPD burden to enhance the statistical power of these studies.



## Acknowledgements

Sponsored by the EURETINA Retinal Medicine Clinical Research Grant.

R.S., C.E., and A.T. received a proportion of their financial support from the UK Department of Health through an award made by the National Institute for Health Research to Moorfields Eye Hospital NHS Foundation Trust and UCL Institute of Ophthalmology for a Biomedical Research Centre for Ophthalmology.

A.P.K is supported by a UK Research and Innovation Future Leaders Fellowship, an Alcon Research Institute Young Investigator Award and a Lister Institute for Preventive Medicine Award. This research was supported by the NIHR Biomedical Research Centre at Moorfields Eye Hospital and the UCL Institute of Ophthalmology.

This work was supported in part by the Said Foundation

We want to acknowledge the participants and investigators of the FinnGen study.

For the purpose of open access, the author has applied a Creative Commons Attribution (CC BY) licence to any Author Accepted Manuscript version arising

1. Ferris FL, Wilkinson CP, Bird A, et al. Clinical Classification of Age-related Macular Degeneration. *Ophthalmology*. 2013;120(4):844-851. doi:10.1016/j.ophtha.2012.10.036
2. Age-Related Eye Disease Study Research Group. The Age-Related Eye Disease Study Severity Scale for Age-Related Macular Degeneration: AREDS Report No. 17. *Archives of Ophthalmology*. 2005;123(11):1484-1498. doi:10.1001/archophth.123.11.1484
3. Zweifel SA, Spaide RF, Curcio CA, Malek G, Imamura Y. Reticular Pseudodrusen Are Subretinal Drusenoid Deposits. *Ophthalmology*. 2010;117(2):303-312.e1. doi:10.1016/j.ophtha.2009.07.014
4. Oak ASW, Messinger JD, Curcio CA. Subretinal Drusenoid Deposits: Further Characterization by Lipid Histochemistry. *Retina*. 2014;34(4):825-826. doi:10.1097/IAE.000000000000121
5. Anderson DMG, Kotnala A, Migas LG, et al. Lysolipids are prominent in subretinal drusenoid deposits, a high-risk phenotype in age-related macular degeneration. *Front Ophthalmol*. 2023;3:1258734. doi:10.3389/fopht.2023.1258734
6. Hogg RE, Silva R, Staurenghi G, et al. Clinical Characteristics of Reticular Pseudodrusen in the Fellow Eye of Patients with Unilateral Neovascular Age-Related Macular Degeneration. *Ophthalmology*. 2014;121(9):1748-1755. doi:10.1016/j.ophtha.2014.03.015
7. Ravera V, Bottoni F, Giani A, Cigada M, Staurenghi G. RETINAL ANGIOMATOUS PROLIFERATION DIAGNOSIS: A Multiimaging Approach. *Retina*. 2016;36(12):2274-2281. doi:10.1097/IAE.0000000000001152
8. Roy Schwartz. Reticular pseudodrusen load is associated with an increased risk of stroke. *Unpublished manuscript*. Published online 2024.
9. Thomson RJ, Chazaro J, Otero-Marquez O, et al. SUBRETINAL DRUSENOID DEPOSITS AND SOFT DRUSEN: Are They Markers for Distinct Retinal Diseases? *Retina*. 2022;42(7):1311-1318. doi:10.1097/IAE.0000000000003460
10. Alexander SL, Linde-Zwirble WT, Werther W, et al. Annual rates of arterial thromboembolic events in medicare neovascular age-related macular degeneration patients. *Ophthalmology*. 2007;114(12):2174-2178. doi:10.1016/j.ophtha.2007.09.017
11. Duan Y, Mo J, Klein R, et al. Age-related macular degeneration is associated with incident myocardial infarction among elderly Americans. *Ophthalmology*. 2007;114(4):732-737. doi:10.1016/j.ophtha.2006.07.045

12. Keilhauer CN, Fritsche LG, Guthoff R, Haubitz I, Weber BH. Age-related macular degeneration and coronary heart disease: evaluation of genetic and environmental associations. *Eur J Med Genet*. 2013;56(2):72-79. doi:10.1016/j.ejmg.2012.10.005
13. Wang J, Xue Y, Thapa S, Wang L, Tang J, Ji K. Relation between Age-Related Macular Degeneration and Cardiovascular Events and Mortality: A Systematic Review and Meta-Analysis. *Biomed Res Int*. 2016;2016:8212063. doi:10.1155/2016/8212063
14. Fernandez AB, Panza GA, Cramer B, Chatterjee S, Jayaraman R, Wu WC. Age-Related Macular Degeneration and Incident Stroke: A Systematic Review and Meta-Analysis. *PLoS One*. 2015;10(11):e0142968. doi:10.1371/journal.pone.0142968
15. Zweifel SA, Imamura Y, Freund KB, Spaide RF. Multimodal fundus imaging of pseudoxanthoma elasticum. *Retina*. 2011;31(3):482-491. doi:10.1097/IAE.0b013e3181f056ce
16. Borooh S, Papastavrou V, Lando L, et al. Reticular Pseudodrusen in Late-Onset Retinal Degeneration. *Ophthalmology Retina*. 2020;5(10):1043-1051. doi:10.1016/j.oret.2020.12.012
17. Aleman TS, Garrity ST, Brucker AJ. Retinal structure in vitamin A deficiency as explored with multimodal imaging. *Doc Ophthalmol*. 2013;127(3):239-243. doi:10.1007/s10633-013-9403-0
18. Seddon JM, Cote J, Page WF, Aggen SH, Neale MC. The US twin study of age-related macular degeneration: relative roles of genetic and environmental influences. *Arch Ophthalmol*. 2005;123(3):321-327. doi:10.1001/archopht.123.3.321
19. Fritsche LG, Igl W, Bailey JNC, et al. A large genome-wide association study of age-related macular degeneration highlights contributions of rare and common variants. *Nature Genetics*. 2016;48(2):134-143. doi:10.1038/ng.3448
20. Edwards AO. Complement Factor H Polymorphism and Age-Related Macular Degeneration. *Science*. 2005;308(5720):421-424. doi:10.1126/science.1110189
21. Hageman GS, Anderson DH, Johnson LV, et al. A common haplotype in the complement regulatory gene factor H (HF1/CFH) predisposes individuals to age-related macular degeneration. *Proc Natl Acad Sci U S A*. 2005;102(20):7227-7232. doi:10.1073/pnas.0501536102
22. Haines JL, Hauser MA, Schmidt S, et al. Complement factor H variant increases the risk of age-related macular degeneration. *Science*. 2005;308(5720):419-421. doi:10.1126/science.1110359
23. Klein RJ, Zeiss C, Chew EY, et al. Complement Factor H Polymorphism in Age-Related Macular Degeneration. 2005;308:6.

24. Zareparsari S, Branham KEH, Li M, et al. Strong association of the Y402H variant in complement factor H at 1q32 with susceptibility to age-related macular degeneration. *Am J Hum Genet.* 2005;77(1):149-153. doi:10.1086/431426
25. Weeks DE, Conley YP, Tsai HJ, et al. Age-Related Maculopathy: A Genomewide Scan with Continued Evidence of Susceptibility Loci within the 1q31, 10q26, and 17q25 Regions. *Am J Hum Genet.* 2004;75(2):174-189.
26. Kenealy SJ, Schmidt S, Agarwal A, et al. Linkage analysis for age-related macular degeneration supports a gene on chromosome 10q26. *Mol Vis.* 2004;10:57-61.
27. Yang Z, Camp NJ, Sun H, et al. A variant of the HTRA1 gene increases susceptibility to age-related macular degeneration. *Science.* 2006;314(5801):992-993. doi:10.1126/science.1133811
28. Shughoury A, Sevgi DD, Ciulla TA. Molecular Genetic Mechanisms in Age-Related Macular Degeneration. *Genes.* 2022;13(7):1233. doi:10.3390/genes13071233
29. DeAngelis MM, Owen LA, Morrison MA, et al. Genetics of age-related macular degeneration (AMD). *Human Molecular Genetics.* 2017;26(R1):R45-R50. doi:10.1093/hmg/ddx228
30. Klein R, Meuer SM, Knudtson MD, Iyengar SK, Klein BEK. The epidemiology of retinal reticular drusen. *American Journal of Ophthalmology.* 2008;145(2):317-326.e1. doi:10.1016/j.ajo.2007.09.008
31. Smith RT, Merriam JE, Sohrab MA, et al. Complement factor h 402H variant and reticular macular disease. *Archives of Ophthalmology.* 2011;129(8):1061-1066. doi:10.1001/archophthamol.2011.212
32. Ueda-Arakawa N, Ooto S, Nakata I, et al. Prevalence and genomic association of reticular pseudodrusen in age-related macular degeneration. *American Journal of Ophthalmology.* 2013;155(2):260-269.e2. doi:10.1016/j.ajo.2012.08.011
33. Puche N, Blanco-Garavito R, Richard F, et al. GENETIC AND ENVIRONMENTAL FACTORS ASSOCIATED WITH RETICULAR PSEUDODRUSEN IN AGE-RELATED MACULAR DEGENERATION. *Retina.* 2013;33(5):998-1004. doi:10.1097/iae.0b013e31827b6483
34. Joachim N, Mitchell P, Rochtchina E, Tan AG, Wang JJ. Incidence and progression of reticular drusen in age-related macular degeneration: findings from an older Australian cohort. *Ophthalmology.* 2014;121(4):917-925. doi:10.1016/j.ophtha.2013.10.043
35. Yoneyama S, Sakurada Y, Mabuchi F, et al. Genetic and clinical factors associated with reticular pseudodrusen in exudative age-related macular degeneration. *Graefes Arch Clin Exp Ophthalmol.* 2014;52(9):1435-1441. doi:10.1007/s00417-014-2601-y

36. Boddu S, Lee MD, Marsiglia M, Marmor M, Freund KB, Smith RT. Risk factors associated with reticular pseudodrusen versus large soft drusen. *American Journal of Ophthalmology*. 2014;157(5):985-993.e2. doi:10.1016/j.ajo.2014.01.023
37. Finger RP, Chong E, McGuinness MB, et al. Reticular Pseudodrusen and Their Association with Age-Related Macular Degeneration. *Ophthalmology*. 2016;123(3):599-608. doi:10.1016/j.optha.2015.10.029
38. Buitendijk GHS, Hooghart AJ, Brussee C, et al. Epidemiology of Reticular Pseudodrusen in Age-Related Macular Degeneration: The Rotterdam Study. *Invest Ophthalmol Vis Sci*. 2016;57(13):5593. doi:10.1167/iovs.15-18816
39. Wu Z, Ayton LN, Luu CD, Baird PN, Guymer RH. Reticular Pseudodrusen in Intermediate Age-Related Macular Degeneration: Prevalence, Detection, Clinical, Environmental, and Genetic Associations. *Invest Ophthalmol Vis Sci*. 2016;57(3):1310. doi:10.1167/iovs.15-18682
40. Lin LY, Zhou Q, Hagstrom S, et al. Association of Single-Nucleotide Polymorphisms in Age-Related Macular Degeneration With Pseudodrusen: Secondary Analysis of Data From the Comparison of AMD Treatments Trials. *JAMA Ophthalmol*. 2018;136(6):682-688. doi:10.1001/jamaophthalmol.2018.1231
41. Domalpally A, Agrón E, Pak JW, et al. Prevalence, Risk, and Genetic Association of Reticular Pseudodrusen in Age-related Macular Degeneration. *Ophthalmology*. Published online July 2019. doi:10.1016/j.optha.2019.07.022
42. Dutheil C, Le Goff M, Cougnard-Grégoire A, et al. Incidence and Risk Factors of Reticular Pseudodrusen Using Multimodal Imaging. *JAMA Ophthalmol*. 2020;138(5):467-477. doi:10.1001/jamaophthalmol.2020.0266
43. Altay L, Liakopoulos S, Berghold A, Rosenberger KD, Ernst A, de Breuk. Genetic and environmental risk factors for reticular pseudodrusen in the EUGENDA study. *Mol Vis*. 2021;27:757-767.
44. Schwartz R, Khalid H, Liakopoulos S, et al. A Deep Learning Framework for the Detection and Quantification of Reticular Pseudodrusen and Drusen on Optical Coherence Tomography. *Transl Vis Sci Technol*. 2022;11(12):3. doi:10.1167/tvst.11.12.3
45. Zweifel SA, Imamura Y, Spaide TC, Fujiwara T, Spaide RF. Prevalence and significance of subretinal drusenoid deposits (reticular pseudodrusen) in age-related macular degeneration. *Ophthalmology*. 2010;117(9):1775-1781. doi:10.1016/j.optha.2010.01.027
46. Ueda-Arakawa N, Ooto S, Tsujikawa A, Yamashiro K, Oishi A, Yoshimura N. Sensitivity and specificity of detecting reticular pseudodrusen in multimodal imaging in Japanese patients. *Retina (Philadelphia, Pa)*. 2013;33(3):490-497. doi:10.1097/IAE.0b013e318276e0ae



47. Bycroft C, Freeman C, Petkova D, et al. The UK Biobank resource with deep phenotyping and genomic data. *Nature*. 2018;562(7726):203-209. doi:10.1038/s41586-018-0579-z
48. Winkler TW, Grassmann F, Brandl C, et al. Genome-wide association meta-analysis for early age-related macular degeneration highlights novel loci and insights for advanced disease. *BMC Med Genomics*. 2020;13(1):120. doi:10.1186/s12920-020-00760-7
49. Holliday EG, Smith AV, Cornes BK, et al. Insights into the genetic architecture of early stage age-related macular degeneration: a genome-wide association study meta-analysis. *PLoS One*. 2013;8(1):e53830. doi:10.1371/journal.pone.0053830
50. Watanabe K, Taskesen E, van Bochoven A, Posthuma D. Functional mapping and annotation of genetic associations with FUMA. *Nat Commun*. 2017;8(1):1826. doi:10.1038/s41467-017-01261-5
51. Ratnapriya R, Sosina OA, Starostik MR, et al. Retinal transcriptome and eQTL analyses identify genes associated with age-related macular degeneration. *Nat Genet*. 2019;51(4):606-610. doi:10.1038/s41588-019-0351-9
52. Ghousaini M, Mountjoy E, Carmona M, et al. Open Targets Genetics: systematic identification of trait-associated genes using large-scale genetics and functional genomics. *Nucleic Acids Res*. 2021;49(D1):D1311-D1320. doi:10.1093/nar/gkaa840
53. Mountjoy E, Schmidt EM, Carmona M, et al. An open approach to systematically prioritize causal variants and genes at all published human GWAS trait-associated loci. *Nat Genet*. 2021;53(11):1527-1533. doi:10.1038/s41588-021-00945-5
54. The GTEx Consortium atlas of genetic regulatory effects across human tissues. *Science*. 2020;369(6509):1318-1330. doi:10.1126/science.aaz1776
55. Kurki MI, Karjalainen J, Palta P, et al. FinnGen provides genetic insights from a well-phenotyped isolated population. *Nature*. 2023;613(7944):508-518. doi:10.1038/s41586-022-05473-8
56. FinnGenn (H7\_AMD, release 10). Accessed July 1, 2024. [https://risteys.finregistry.fi/endpoints/H7\\_AMD](https://risteys.finregistry.fi/endpoints/H7_AMD)
57. Mbatchou J, Barnard L, Backman J, et al. Computationally efficient whole-genome regression for quantitative and binary traits. *Nat Genet*. 2021;53(7):1097-1103. doi:10.1038/s41588-021-00870-7
58. Bulik-Sullivan BK, Loh PR, Finucane HK, et al. LD Score regression distinguishes confounding from polygenicity in genome-wide association studies. *Nat Genet*. 2015;47(3):291-295. doi:10.1038/ng.3211
59. Pre-calculated LD scores for European ancestry. [https://data.broadinstitute.org/alkesgroup/LDSCORE/eur\\_w\\_ld\\_chr.tar.bz2](https://data.broadinstitute.org/alkesgroup/LDSCORE/eur_w_ld_chr.tar.bz2)

60. R Core Team. *R: A Language and Environment for Statistical Computing*. R Foundation for Statistical Computing; 2017. <https://www.R-project.org/>
61. Giambartolomei C, Vukcevic D, Schadt EE, et al. Bayesian Test for Colocalisation between Pairs of Genetic Association Studies Using Summary Statistics. *PLOS Genetics*. 2014;10(5):e1004383. doi:10.1371/journal.pgen.1004383
62. Wallace C. Eliciting priors and relaxing the single causal variant assumption in colocalisation analyses. *PLOS Genetics*. 2020;16(4):e1008720. doi:10.1371/journal.pgen.1008720
63. Wallace C. A more accurate method for colocalisation analysis allowing for multiple causal variants. *PLOS Genetics*. 2021;17(9):e1009440. doi:10.1371/journal.pgen.1009440
64. Landau WM. The targets R package: a dynamic Make-like function-oriented pipeline toolkit for reproducibility and high-performance computing. *Journal of Open Source Software*. 2021;6(57):2959. doi:10.21105/joss.02959
65. Archetypes for Targets. Accessed September 12, 2024. <https://docs.ropensci.org/tarchetypes/>
66. Wickham H, Averick M, Bryan J, et al. Welcome to the Tidyverse. *Journal of Open Source Software*. 2019;4(43):1686. doi:10.21105/joss.01686
67. Blischak JD, Carbonetto P, Stephens M. Creating and sharing reproducible research code the workflowr way. Published online October 14, 2019. doi:10.12688/f1000research.20843.1
68. Gohel D, ArData, Jager C, et al. flextable: Functions for Tabular Reporting. Published online May 5, 2024. Accessed September 12, 2024. <https://cran.r-project.org/web/packages/flextable/index.html>
69. Sjoberg DD, Whiting K, Curry M, Lavery JA, Larmarange J. Reproducible Summary Tables with the gtsummary Package. *The R Journal*. 2021;13(1):570-580.
70. knitr - Yihui Xie | 谢益辉. Accessed September 12, 2024. <https://yihui.org/knitr/>
71. Jabbarpoor Bonyadi MH, Yaseri M, Nikkhah H, Bonyadi M, Soheilian M. Association of risk genotypes of ARMS2/LOC387715 A69S and CFH Y402H with age-related macular degeneration with and without reticular pseudodrusen: a meta-analysis. *Acta Ophthalmol*. 2018;96(2):e105-e110. doi:10.1111/aos.13494
72. Smith RT, Sohrab MA, Busuioc M, Barile G. Reticular macular disease. *American Journal of Ophthalmology*. 2009;148(5):733-743.e2. doi:10.1016/j.ajo.2009.06.028
73. Fritsche LG, Loenhardt T, Janssen A, et al. Age-related macular degeneration is associated with an unstable ARMS2 (LOC387715) mRNA. *Nat Genet*. 2008;40(7):892-896. doi:10.1038/ng.170

74. Curcio CA, Messinger JD, Sloan KR, McGwin G, Medeiros NE, Spaide RF. Subretinal Drusenoid Deposits In Non-Neovascular Age-Related Macular Degeneration: Morphology, Prevalence, Topography, And Biogenesis Model. *Retina*. 2013;33(2):10.1097/IAE.0b013e31827e25e0. doi:10.1097/IAE.0b013e31827e25e0
75. Kanda A, Chen W, Othman M, et al. A variant of mitochondrial protein LOC387715/ARMS2, not HTRA1, is strongly associated with age-related macular degeneration. *Proceedings of the National Academy of Sciences*. 2007;104(41):16227-16232. doi:10.1073/pnas.0703933104
76. Kortvely E, Hauck SM, Duetsch G, et al. ARMS2 Is a Constituent of the Extracellular Matrix Providing a Link between Familial and Sporadic Age-Related Macular Degenerations. *Investigative Ophthalmology & Visual Science*. 2010;51(1):79-88. doi:10.1167/iovs.09-3850
77. Xu YT, Wang Y, Chen P, Xu HF. Age-related maculopathy susceptibility 2 participates in the phagocytosis functions of the retinal pigment epithelium. *International Journal of Ophthalmology*. 2012;5(2):125-132. doi:10.3980/j.issn.2222-3959.2012.02.02
78. A J, S K, N Z, et al. Increased expression of multifunctional serine protease, HTRA1, in retinal pigment epithelium induces polypoidal choroidal vasculopathy in mice. *Proceedings of the National Academy of Sciences of the United States of America*. 2011;108(35). doi:10.1073/pnas.1102853108
79. Kumar S, Berriochoa Z, Ambati BK, Fu Y. Angiographic features of transgenic mice with increased expression of human serine protease HTRA1 in retinal pigment epithelium. *Invest Ophthalmol Vis Sci*. 2014;55(6):3842-3850. doi:10.1167/iovs.13-13111
80. Yang Z, Tong Z, Chen Y, et al. Genetic and functional dissection of HTRA1 and LOC387715 in age-related macular degeneration. *PLoS Genet*. 2010;6(2):e1000836. doi:10.1371/journal.pgen.1000836
81. Williams BL, Seager NA, Gardiner JD, et al. Chromosome 10q26–driven age-related macular degeneration is associated with reduced levels of *HTRA1* in human retinal pigment epithelium. *Proc Natl Acad Sci USA*. 2021;118(30):e2103617118. doi:10.1073/pnas.2103617118
82. Alliance of Genome Resources - PARD3B. Accessed July 18, 2024. <https://www.alliancegenome.org/gene/RGD:1584992>
83. Alliance of Genome Resources - ITPR1. Accessed July 18, 2024. <https://www.alliancegenome.org/gene/HGNC:6180>
84. Dentici ML, Barresi S, Nardella M, et al. Identification of novel and hotspot mutations in the channel domain of ITPR1 in two patients with Gillespie syndrome. *Gene*. 2017;628:141-145. doi:10.1016/j.gene.2017.07.017

85. Alliance of Genome Resources - SLN. Accessed July 18, 2024.

<https://www.alliancegenome.org/gene/HGNC:11089>

86. Common and rare variants in patients with early onset drusen maculopathy - Breuk - 2022 - Clinical Genetics - Wiley Online Library. Accessed September 12, 2024.

<https://onlinelibrary.wiley.com/doi/10.1111/cge.14212>